

## Acoustic graded-index lenses

著者	櫛引 淳一
journal or publication title	Applied Physics Letters
volume	59
number	12
page range	1398-1400
year	1991
URL	<a href="http://hdl.handle.net/10097/46344">http://hdl.handle.net/10097/46344</a>

doi: 10.1063/1.105318

## Acoustic graded-index lenses

C. K. Jen, Z. Wang, A. Nicolle,<sup>a)</sup> C. Neron, E. L. Adler,<sup>a)</sup> and J. Kushibiki<sup>b)</sup>  
*IMI, National Research Council, Boucherville, Quebec J4B 6Y4, Canada*

(Received 11 February 1991; accepted for publication 19 June 1991)

Experimental investigations of the focusing behavior of rods having acoustically graded-index profile across the rod diameter are presented for the first time. The ray acoustics approach is used for the theoretical interpretation. Acoustic velocity profiles have been measured using a 225 MHz line focus beam scanning acoustic microscope. The focusing behavior is visualized with a Schlieren system.

Glass rods having a graded index of refraction along the radial direction are commonly used in optical lens design. They are named graded-index (GRIN) lenses<sup>1</sup> or SELFOC (self-focusing) rods.<sup>2</sup> The parameters that define the index distribution provide valuable new degrees of freedom for designers of optical imaging systems.<sup>1</sup> The techniques to fabricate such GRIN lenses or SELFOC rods are ion exchange, chemical vapor deposition, sol-gel, etc. Such lenses are commercially available.

This work is the first report to demonstrate that rods having acoustically graded-index (velocity) profiles exhibit focusing behaviors in acoustics similar to those optical GRIN rods exhibit in optics. We name them "acoustic GRIN rods or lenses." For lens applications, the phase velocity at the center of either optical or acoustic GRIN rod must be less than that at the edge. One application of acoustic GRIN rods is for long acoustic imaging probes.<sup>3</sup> The fabrication methods for optical GRIN rods may also be used to produce acoustic GRIN rods. It is noted that optically opaque materials may be employed for acoustic rods. Furthermore, in optics only a transverse wave is involved, whereas in acoustics, both transverse (shear) and longitudinal waves should be considered. However, in this presentation experimental results for only longitudinal waves are given.

The GRIN acoustic rods used for this study were made by a modified chemical vapor deposition (MCVD) method.<sup>4</sup> In our previous studies<sup>5</sup> on the acoustic characterization of doped silica clad fibers fabricated by the same MCVD method, we have shown that such rods having graded optical refractive index profiles also exhibit graded acoustic velocity variations. However, proper dopants must be chosen in order to meet the lens focusing criterion that the phase velocity at the center is less than that at the edge. Based on our previous studies<sup>5</sup> we fabricated several acoustic GRIN rods for this study. For isotropic materials such as silica glasses, longitudinal and shear waves are normally used for acoustic characterization. Since it is very difficult to obtain the radial distribution of bulk longitudinal,  $v_L$ , and shear wave velocity,  $v_S$ , for small diameter rods, an approach which uses the reflection scanning acoustic microscopy (SAM) and  $V(z)$  technique to obtain leaky surface acoustic wave (LSAW) and leaky surface-skimming compressional wave

(LSSCW) velocities<sup>5,6</sup> is adopted here. Because LSAW and LSSCW have predominantly shear and longitudinal wave components, respectively, their velocity profiles can be regarded as those of  $v_S$  and  $v_L$ .

We have previously reported such measurements using a 775 MHz point focus beam (PFB) SAM,<sup>5</sup> here a 225 MHz line focus beam (LFB) SAM (Ref. 6) is used. The velocity measured was along the direction perpendicular to the LFB and parallel to the radial direction of the rod. Our 775 MHz PFB SAM offers better spatial resolution, but the 225 MHz LFB SAM provides higher accuracy in velocity measurements due to the higher signal-to-noise ratio especially for LSSCW. Due to the defocusing requirement of  $V(z)$  measurements, the measured velocity represents an average value over the defocused area which is about 50 by 1000  $\mu\text{m}$  for the LFB SAM. All the samples for the LFB SAM were polished; the last and the finest polishing step was with a mechanical-chemical (0.06  $\mu\text{m}$ ) polishing. The relative accuracy in  $v_{\text{LSAW}}$  (average value) profile measurements is better than 0.1%. Since the LSSCW is very weakly excited, the signal-to-noise ratio for such a wave is much less than that for LSAW, hence, less accuracy is available in  $v_{\text{LSSCW}}$  measurements. More studies are required in order to understand the effects of graded velocity profiles on the measurement accuracy. However, detailed descriptions for the  $V(z)$  measurement of the LFB SAM is given in Ref. 6.

Figures 1(a) and 1(b) show the measured  $v_{\text{LSAW}}$  and  $v_{\text{LSSCW}}$ , respectively, for three acoustic GRIN rods designated as A (\*), B (○) and C (△) with different dopant concentrations and distributions. All the GRIN rods have a diameter of  $\sim 5$  mm but only A and B have a cladding with a thickness of  $\sim 2.5$  mm. The optical refractive index profile shown in Fig. 2 of the rod C has been measured by a commercial (York Technology) device which provides spatial resolution better than 10  $\mu\text{m}$ . The abrupt refractive index variation at the rod center and the minor oscillations across the GRIN rod are due to the modified chemical vapor deposition fabrication process.<sup>4</sup> GRIN rods made by other techniques do not normally have such dips and fine structures. Since the LFB SAM only measures the average velocity over a 40 by 1000  $\mu\text{m}$  area and the measurements have been taken at a distance of 0.1 mm/step, the fine details of the profile appearing in Fig. 2 cannot be seen in the curve C of Figs. 1(a) and 1(b). However, with a high spatial resolution PFB SAM the abrupt change at the rod center can be seen.<sup>5</sup> Rods A and B have similar center dips and fine structures as rod C. It is interesting to note that

<sup>a)</sup>Department of Electrical Eng., McGill University, Montreal, Quebec H3A 2A7, Canada.

<sup>b)</sup>Department of Electrical Eng., Tohoku University, Sendai 980, Japan.

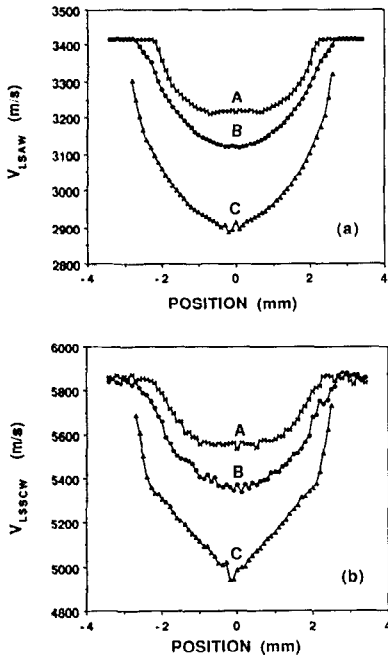


FIG. 1. The measured (a)  $v_{LSAW}$  and (b)  $v_{LSSCW}$  profiles of the GRIN rods A, B, and C.

the refractive index difference between the maximum and the minimum of the rod C is about 2%, whereas the acoustic velocity difference is about 15%. Furthermore, the dips in refractive index profiles for rods A, B, and C correspond to the peaks in the corresponding acoustic velocity profiles.

The focusing mechanisms of optical GRIN lenses have commonly been explained by the ray optics theory.<sup>1</sup> The main difference between the ray optics and ray acoustics is that there exist both longitudinal and shear acoustic waves but only transverse (shear) optical waves in an isotropic material. In an isotropic and inhomogeneous materials such as GRIN rods these two acoustic waves couple to each other due to mode conversion. A sharper variation of an acoustic velocity profile means a stronger coupling be-

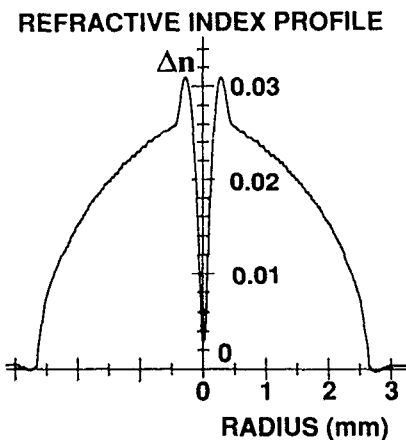


FIG. 2. The measured optical refractive index profile of the rod C.

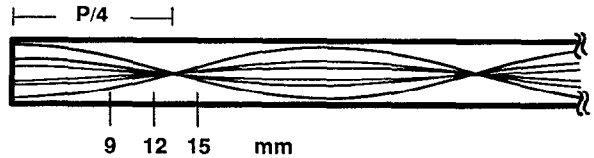


FIG. 3. Acoustic rays in an acoustic GRIN rod.

tween two such waves. If the profile of a GRIN acoustic rod does not have abrupt variations comparing to the acoustic wavelength and the rod diameter is large (i.e., more than tens of acoustic wavelengths), it is expected that ray acoustics can be used to approximately interpret the acoustic focusing behaviors. Because of this consideration and available experimental instrumentation, a longitudinal acoustic transducer operating at 50 MHz is used for the experiments described below. It means that the diameters of GRIN rods A, B, and C are about 40 longitudinal acoustic wavelengths.

For optical GRIN lenses the refractive profiles often vary parabolically as a function of radius. The index variation may be expressed as<sup>1</sup>

$$n(r) = n_0(1 - Qr^2)^{1/2} \sim n_0(1 - Qr^2/2), \quad (1)$$

where  $n_0$  is the refractive index at the rod center,  $Q$  is a positive constant, and  $r$  is the radial distance from the rod axis. As a result of the parabolic index variation a ray incident on the front surface follows a sinusoidal path along the rod lens. The period of this sinusoidal path is called the "pitch" of the lens and is an important parameter in GRIN lens imaging and is given by  $P = 2\pi/\sqrt{Q}$ .

Let us express the velocity profile of GRIN acoustic rods as

$$\frac{1}{v_L(r)} = \frac{1}{v_{L0}}(1 - Q_a r^m)^{1/2} \sim \frac{1}{v_{L0}}(1 - Q_a r^m/2), \quad (2)$$

where  $Q_a$  is a positive constant,  $m$  is the order of the power of the radius, and  $v_{L0}$  is the velocity at the rod center. For a GRIN acoustic rod with a parabolic profile (i.e.,  $m=2$ ), acoustic rays shown in Fig. 3 behave similarly as optical rays behave in optical GRIN rods.<sup>1</sup> If we assume  $v_{LSSCW} = v_L$ , for rod B the approximate values for  $m$  and  $Q_a$  are 2.6 and  $0.020/\text{mm}^2$ , respectively. Thus, the expected pitch  $P$  is about 45 mm.

A standard Schlieren system is used to visualize the acoustic waves exiting from the rods immersed in a water tank. Rods A, B, C, and a Pyrex rod with a uniform velocity distribution across the rod diameter are used in the experiments. The two faces of each rod are polished. A 50 MHz longitudinal ultrasonic transducer of 6.35 mm diam is bonded to one face and the longitudinal acoustic waves coming out of the other face are monitored by the visualization system.

To assure a uniform insonification a 6-mm-thick and 10-mm-diam Pyrex rod was used for the experiment. The acoustic waves coming out of this rod into the water were indeed very uniform. Figures 4(a)–4(c) show the acoustic

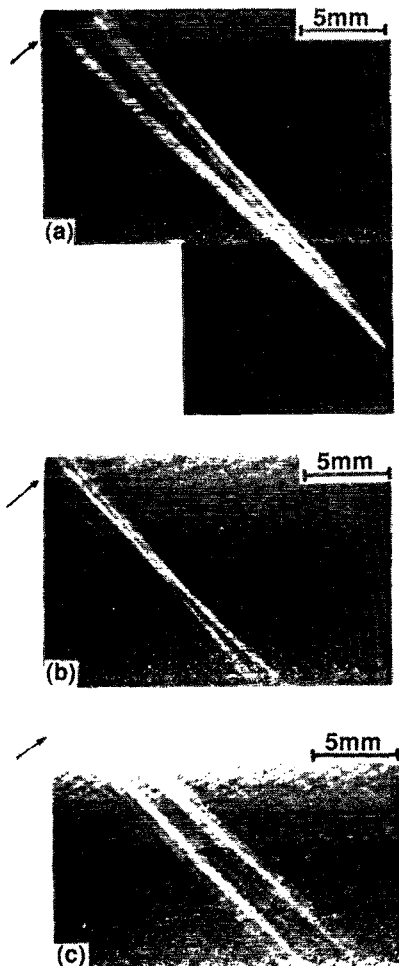


FIG. 4. Images of acoustic waves coming out of type B rod with a thickness of (a) 9, (b) 12, and (c) 15 mm, respectively, into the water. Arrow indicates the rod-water interface.

waves coming out of type B rods of 9, 12, and 15 mm thickness, respectively. It is noted that, due to the abrupt velocity change at the rod center mentioned previously, the acoustic wave energy is not concentrated at the rod center implying that the focusing beams are not formed by a solid cone but rather by a hollow one. Therefore, in Figs. 4(a)–4(b) we see a stronger beam intensity away from the center.

Using the acoustic ray illustration we expect to see several features of the acoustic focusing mechanisms of the acoustic GRIN rod B with these three different thicknesses indicated in Fig. 3. Figure 4(b) indicates a shorter focal length than that in Fig. 4(a) and also shows the diverging beams in addition to the converging beams. Due to the high acoustic attenuation in water, the diverging beam in

Fig. 4(a) after the focal point is too weak to be seen. The diverging behavior of acoustic rays at a given position of the GRIN rod shown in Fig. 3 can be verified in Fig. 4(c). It is noted that the acoustic rays in Figs. 4(a)–4(c) are in the water. They are different from the ray traces illustrated in Fig. 3 due to the Snell law at the rod-water interface. From Figs. 4(a)–4(c) we estimate that the pitch  $P$  for the GRIN rod B is about 52 mm. The difference between the measured pitch of 52 mm and the expected value of 45 mm from Fig. 1 and Eq. (2) is believed to be caused by the nonideal graded velocity profile such as the abrupt change at the rod center and nonparabolic ( $m = 2.6$ ) profile, measurement accuracy of  $v_{LSSCW}$ , and its deviation from  $v_L$ .

Figures 1(a) and 1(b) indicate that rod B has a sharper velocity variation than rod A. With a thickness of 12 mm, from the ray acoustics approximation we expect that the focal length of rod A is longer than that of rod B, as shown in Fig. 4(b). We have performed an experiment and confirmed this theoretical expectation. Through many similar experiments we conclude that a ray acoustics interpretation works reasonably well for rods A, B, and C shown in Fig. 1. We also believe that claddings of rods A and B have little effects on the measurement data presented in Figs. 4(a)–4(c). Moreover, the shear acoustic waves in these GRIN rods also exhibit similar focusing behaviors which will be reported elsewhere.

The focusing behaviors of acoustic GRIN rods have been experimentally demonstrated for the first time. The ray acoustics approach is used for the theoretical interpretation. Acoustic velocity profiles were measured using a 225 MHz line focus beam scanning acoustic microscope. The focusing behavior is visualized with a Schlieren system. Such rods can be used to provide valuable new degrees of freedom for designers of acoustic lenses, buffer rods,<sup>3</sup> and imaging systems. They can also be made of optically opaque materials such as metals and ceramics.

This work is partially supported by the Natural Sciences and Engineering Research Council of Canada. The GRIN acoustic rods were provided by L. Bonnell and K. Abe at the National Institute of Optics, Sainte-Foy, Quebec.

<sup>1</sup>E. W. Marchand, *Gradient Index Optics* (Academic, New York, 1978).

<sup>2</sup>T. Uchida, M. Furukawa, I. Kitano, K. Koizumi, and H. Matsumura, *IEEE J. Quantum. Electron.* **QE-6**, 606 (1970).

<sup>3</sup>C. K. Jen, C. Neron, E. L. Adler, G. W. Farnell, J. Kushibiki, and K. Abe, *Proc. IEEE Ultrason. Symp.*, 90CH2938-9, 875 (1990).

<sup>4</sup>W. G. French, R. E. Jaeger, J. B. Macchesney, S. R. Nagel, K. Nassau, and A. D. Pearson, in *Optical Fiber Telecommunications*, edited by S. E. Miller and A. G. Chynoweth (Academic, New York, 1979), pp. 233–261.

<sup>5</sup>C. K. Jen, C. Neron, J. F. Bussiere, L. Li, R. Lowe, and J. Kushibiki, *Appl. Phys. Lett.* **55**, 2485 (1989).

<sup>6</sup>J. Kushibiki and N. Chubachi, *IEEE Trans. Sonics Ultrason.* **SU-32**, 189 (1985).